JEE Journal of Ecological Engineering

Journal of Ecological Engineering, 2026, 27(4), 244–257
https://doi.org/10.12911/22998993/214975
ISSN 2299–8993, License CC-BY 4.0

Received: 2025.11.19
Accepted: 2026.02.18
Published: 2026.03.01

Evaluating the removal of malachite green and methyl violet dyes from aqueous environment by three-dimensional electrocoagulation-flotation batch reactor

Zena F. Abdullah[1], Rasha H. Salman[1*]

[1] Department of Chemical Engineering, College of Engineering, University of Baghdad, Baghdad, Iraq
* Corresponding author e-mail: rasha.habeeb@coeng.uobaghdad.edu.iq

ABSTRACT

When dye is present in wastewater, it is considered a hazardous organic pollutant and must be eliminated. The goal of the current study was to evaluate the elimination of Malachite green (MG) and Methyl violet (MV) dyes using Ni foam (NiF) as an anode, along with stainless steel mesh electrodes as cathodes, and alum sludge (AS) as a third particle electrode in a three-dimensional electrocoagulation-flotation system (3DECF). With an electrolysis period of 30 minutes and pH = 7, response surface method was used to estimate the optimum conditions of studied parameters. These parameters were current density within the range of 1–5 mA/cm², concentration of NaCl within the range of 0.4 –1 g/L, and air flow rate within a range of 1–5 L/min. After 30 minutes of electrolysis, a dye removal of 93.151% was achieved at 5 mA/cm², 1 g/L NaCl, and an air flow rate of 3.7 L/min. The energy consumed was 67.847 kWh/kg of dyes. The model for dye removal is highly significant, with an F-value and P-value of 78.63 and 0.000, respectively, and the treatment process can be accurately described by this model. The R^2 multiple correlation value was 0.9930, and there was a very good value of the adj. R^2 (0.9804) and the pred. R^2 (0.8879). EDX and FESEM were applied to examine the morphology of the surface and structure of the NiF electrode and alum sludge. Due to the excellent 3D structure of the foam electrode, this economical 3DECF system with the NiF anode and stainless-steel mesh as the cathode has demonstrated its high effectiveness in removing MG and MV dye with a low amount of NaCl. This makes the foam electrode an excellent choice. The results overall indicate that the 3DECF of dyes in binary systems may be an effective method with positive socioeconomic and environmental impacts. It can also increase efficiency when used in connection with another process.

Keywords: three-dimensional, electrocoagulation-flotation, alum sludge, Ni foam, surface response.

INTRODUCTION

In the past few years, water contamination has attracted significant attention as a global issue. The excessive dumping of domestic, agricultural, and industrial wastewater into freshwater bodies before treatment is causing the water quality to deteriorate daily. For instance, fertilizers and insecticides are used in agriculture to improve crop quality, and the textile industry uses dyes to color textiles (Akhtar et al., 2025; Anbia et al., 2010). The prolonged presence of these substances has posed a serious risk to human health, increasing exposure to cancer, respiratory conditions, elevated heart rate, and other conditions (Hsini et al., 2020; Qadeer et al., 2020).

Dyes are used extensively across many industries (Alegbe and Uthman, 2024; Das et al., 2023). These dyes might be synthetic (Amalina et al., 2022). The structure, applications, color, ionic form, and stability of synthetic dyes can all be used to further categorize them (Chen et al., 2019). Azo and non-azo dyes are two categories of synthetic dyes. Additional classifications for azo dyes include reactive, basic, acid, sulfur, and dispersion. Because of their complex aromatic formula, these dyes are distinguished by molecular stability as well as natural reactivity (Waghchaure et al., 2023). The printing, leather processing, textile, and cosmetic sectors are the primary contributors of synthetic dyes in wastewater (Askari et al., 2023; Seidmohammadi et al.,

2019). In aquaculture, malachite green (MG) dye was widely utilized to prevent and treat fungal and protozoal diseases in fish eggs, fingerlings, and adults. Still, it first gained widespread use in the textile industry (Ismail and Sakai, 2022; Samuchiwal et al., 2021). Methyl violet (MV) is mainly used to create deep violet manners in paint and ink, and as a violet dye for textiles. It serves as a hydration indication as well.

Due to their detrimental effects, numerous physical and chemical approaches have been proposed for wastewater treatment that contains dyes, such as filtration and ultrafiltration (M. Chen et al., 2024), precipitation process (Li et al., 2023), biological decontamination (Derakhshan et al., 2023; Najim and Mohammed, 2018), ion exchange (Jasim and Ajjam, 2024), adsorption (Jawad and Naife, 2022; Lichtmannegger et al., 2024), as well as particle aggregation and flocculation method (Ahmad et al., 2024). Because of the costly nature and tendency to produce secondary pollutants, these approaches are estimated to be inefficient (Crini and Lichtfouse, 2019).

In addition to being inexpensive and simple to install, an electrochemical method is one of the attractive and eco-friendly techniques because it does not emit poisons into the surroundings and does not involve the addition of numerous chemicals (Abbas and Abbas, 2022; Jasim and Salman, 2024). Because it can remove a variety of pollutants, electrocoagulation has drawn a lot of interest among water treatment methods in the 20th century (Islam, 2017).

The foundation of the EC method is the use of sacrificial anodes, which are often made of nickel, iron, or aluminum. Under certain circumstances, these electrodes dissolve in water, generating coagulant species (Alardhi et al., 2023). Equation 1 illustrates how the reduction at the cathode in water produces hydroxyl and hydrogen gas ions, whereas Equation 2 shows how oxidation of water takes place on the anode (Tijana et al., 2021).

$$4H_2O + 4e^- \leftrightarrow 2H_2O_{(g)} + 4OH^-_{(aq)} \quad (1)$$

$$H_2O \leftrightarrow 4H^+_{(aq)} + O_{2(g)} + 4e^- \quad (2)$$

Equations (3–5) show that the anode (M) will dissolve and provide a metal cation (Jasim and Salman, 2024).

$$M \rightarrow M^{n+} + ne^- \quad (3)$$

$$H_2O_{(l)} + 2e^- \rightarrow 2OH^- + H_{2(g)} \quad (4)$$

$$M^{n+} + nOH^- \rightarrow M(OH)_{n(s)} \quad (5)$$

To improve the sustainability and cost-effectiveness of the technique, this study investigated the use of NiF as an electrode in electrocoagulation. The excellent stability, well-defined electrochemical activity, and high specific capacitance of nickel foam make it a desirable material, based on some previous studies (Mohammed Ali and Salman, 2024). Because of its large surface area, metallic foam can be used as a sacrificial anode in the EC process to provide a continuous redox reaction and to catalytically adjust the energy barrier to electron transfer, thereby promoting the formation of metal hydroxides (Muthumanickam and Saravanathamizhan, 2021).

One of the primary goals of the current study was to examine the potential application of electrocoagulation (EC) in combination with macro flotation for the treatment of colored wastewater. Macro flotation was achieved by generating bubbles with a high-quality ceramic diffuser at the base of the EC cell. These bubbles not only assist in mixing and reducing particle settling but also attach to coagulated flocs, causing them to rise to the surface (Abdulrazzaq et al., 2021).

Electrochemical methods based on three-dimensional (3D) electrodes have attracted significant interest. In 3D electrochemical techniques, the particle electrodes play the role of third electrode, in addition to the two electrodes used in conventional (two-dimensional) electrochemical systems. These particle electrodes must be placed between the anode and the cathode. Granular or powdery materials are frequently served as particle electrodes and function as electrodes in 3D electrochemical systems (Theydan et al., 2024). Many researchers have sought an alternative third-particle electrode material that is efficient, low-cost, and sustainable.

In the water treatment facilities that use aluminum salts as coagulants, the drinking water treatment process produces AS as a byproduct. When the $Al_2(SO_4)_3$ coagulant is added to water at a high enough concentration, it combines with hydroxides (OH^-) to form the main component of AS, an amorphous composite of colloidal suspended solids, humic particles, and organic materials, $Al(OH)_3$ (Jo et al., 2021; Kumar et al., 2020). The researchers found that the specific surface area of AS can vary between 21 and 364.55 $m^2.g^{-1}$, or around one-third of the surface area of activated carbon (Zhou and Haynes, 2010).

The main goals of the current study are to use the minimum amount of NaCl possible and a low current while lowering the cost of wastewater treatment using a 3DECF technique using Ni foam as anode. The authors aimed to further enhance the benefits of the electrocoagulation (EC) method by combining a third particle electrode made of alum sludge, utilizing a macro flotation process to remove the MG and MV dyes from an aqueous solution. In the current study, the regulated parameters were optimized using the response surface method (RSM).

MATERIALS AND METHODS

Chemicals

Malachite green (MG) (APHA CHEMIKA, India) and Methyl violet (MV) (Hopkin Williams, ESSEX, England) were the dyes used in this study, and their properties are shown in Table 1. Hydrochloric acid (HCl) (purity of 37%, Thomas Baker Pvt. Ltd., India) and sodium hydroxide (NaOH) (with ≥ 97% of purity) have been purchased from Sigma Central Drug House (p) Ltd., New Delhi-110002 India), which were used to maintain the desired value of pH, and 98% purity of sulfuric acid (H_2SO_4). NaCl and Na_2SO_4 (APHA CHEMIKA, India, with 99.9% purity) were used as supporting electrolytes to increase solution conductivity. Since all components used in this study are highly pure, no additional purification was required, and the aqueous solution was made with distilled water.

3DECF Setup

The dimensions of a novel batch of Perspex rectangular cell were 16 cm in length, 12 cm in width, and 10 cm in height. The initial concentration of methyl violet or malachite green was 25 mg/L for each, 0.025 M of anhydrous sodium sulfate, and 0.4, 0.7, or 1 g/L of sodium chloride were dissolved in distilled water to prepare simulated effluent samples with a total volume of 1.5 L.

The NiF anode dimensions were 16 cm wide, 8.5 cm high, and 1 cm thick, while the SS mesh cathode had the same width and height but was 0.1 cm thick. 6.5 cm of each electrode was submerged in the electrolytic solution, and the active area on both sides of the NiF anode was 208 cm^2. The space between the electrodes was fixed at 3 cm. The NiF and SS mesh were cleaned with 0.1M H_2SO_4 and 0.1M HCl, respectively, to remove any oxide layers on their surfaces, and then were subsequently washed with deionized water.

A macroporous ceramic gas diffuser was used, situated at the base of the cell under the third particle on each side. An air compressor (55W, China) was used to supply air to the solution, and a flow meter with a range of 1–12 L/min was used to control the flow.

A diaphragm made by a three-dimensional printer is introduced between the anode and cathode compartments to control ion migration and prevent unwanted reactions, like colliding with three-dimensional electrodes with the anode and cathode for improving treatment selectivity, electrode longevity, and effluent quality.

Table 1. Properties of the Malachite green (MG) and Methyl violet (MV) dyes

Structure	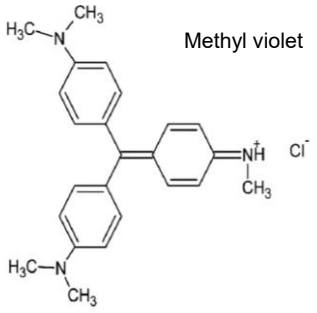 Methyl violet	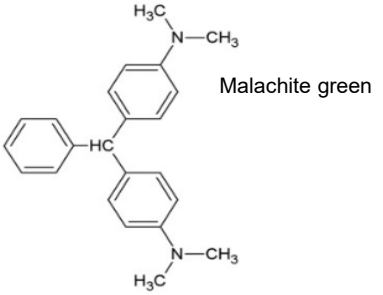 Malachite green
Chemical name	$C_{24}H_{28}N_3Cl$ Triarylmethane dye	$C_{52}H_{54}N_4O_{12}$ Triphenylmethane dye
Molecular mass	394.95 g/mol	927.02 g/mole
Wavelength	584 nm	617 nm
Color	Violet powder or crystals	Bluish green to dark green

Every experiment was carried out at room temperature (27 ± 3°C), replicated, and the average value was calculated. In order to bring the pH of the medium to 7, 0.1M of NaOH and 0.1M of HCl were used. A pH meter (HANNA HI 991001) was used to measure the pH of the samples. A power supply (UNI-T UTP3315PE, 0–30 V, 0–5 A) was used to supply the required current density to the electrodes connected to it. The power source was turned on with the necessary current. Samples were taken from the electrolytic solution at the beginning of the experiment and after 30 minutes of electrolysis. Figure 1 displays the experimental configuration.

The wet sludge cake sample used in this study, which was used as the third particle electrode, was taken from the Karbala Water Filtration Station, a nearby drinking water treatment facility in Iraq. To create particles with a size of 4-4.75 mm, the raw sludge was dried, crushed, sieved, and then dried for 24 hours at 110°C. The sludge that had been calcined for one hour at 600°C in an electrical muffle furnace was analyzed using XRF, EDX, and SEM. The calcination of wet sludge was shown to involve several chemical reactions, such as the crystallization of amorphous silica, the dehydration of colloidal $Al(OH)_3$, and the creation of Al_2O_3. These chemical reactions, therefore, have a significant effect on the microstructure of wet sludge (Nguyen et al., 2023).

A spectrometer (UV-9200, UK) was used to determine the concentration of MV and MG at wavelengths (λ) of 584 nm and 617 nm, respectively. The color removal efficiency was estimated as follows:

$$Removal\ efficiency\ (\%) = \\ = \frac{(C_i - C_t)}{C_i} \times 100\% \quad (6)$$

where: C_i and C_t are the initial and final dyestuff concentrations (mg/L), respectively. Additionally, the chemical oxygen demand COD was measured at the optimum conditions to detect the removal of organics utilizing the Lovibond reactor and detected by the photometer system MD 200. Equation 7 was used to determine the energy consumption required to remove dye from a solution, expressed in kWh/kg of dyestuff removed (Hasnaoui et al., 2024).

$$SEC = \frac{U \times i \times t_{EC}}{(C_i - C_t) \times V} \times 1000 \text{ (kWh/kg)} \quad (7)$$

where: U is the cell voltage (V), i is the applied current (A), t_{EC} is the electrolysis time (h), and V is the volume (L) of the treated solution. C_i and C_t are the initial and final dyestuff concentrations (mg/L), respectively.

Electrode characterization

Field-emission scanning electron microscopy (SEM, FEI-company) and energy dispersive X-ray (EDX, Bruker Company/Germany) was utilized to detect the surface morphology for NiF and alum

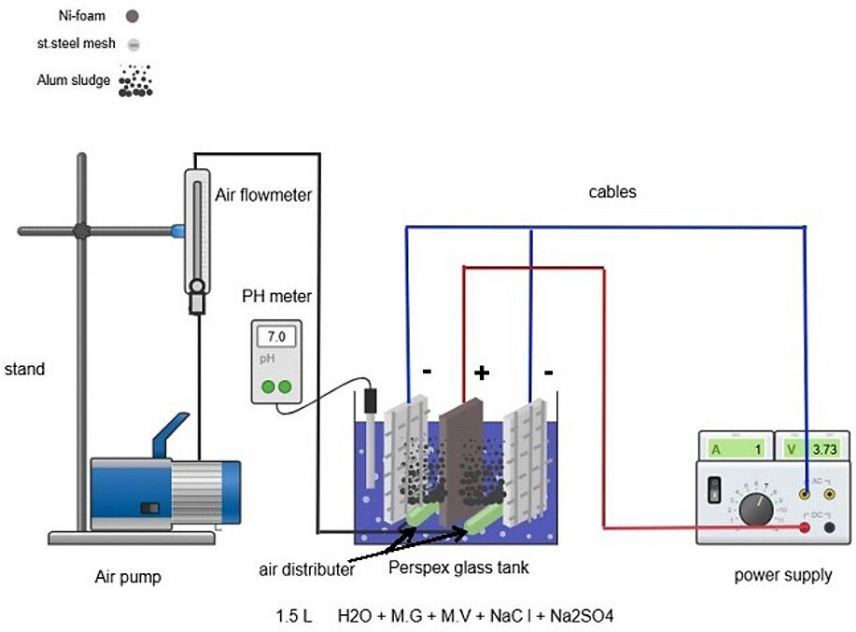

Figure 1. A schematic plot of the 3DECF cell

sludge and the elements composition of NiF electrodes as anode and alum sludge as a third particle before and after its utilization in the 3DECF process as well as an X-ray Fluorescence spectrometer (model XEPOS, type 766004814) for analyzing the composition elements for alum sludge.

Experimental design

RSM is a multivariable technique that is ideal for determining optimal operating parameters and can be used in a theoretical context with a response function in an experimental domain design (Theydan et al., 2024). In the present study, a Box-Behnken design (BBD) was employed to optimize the variables and conduct the design of experiments (DOE). Fifteen tests with three duplicates and a central point were performed using a Box-Behnken (BB) experimental design.

The current density (X_1) with range (1, 3, 5) mA/cm^2, NaCl concentration (X2) with range (0.4, 0.7, 1) g/L, and air flow rate (X3) with range (1, 3, 5) L/min were selected for investigation in a series of tests to estimate the optimal conditions for the removal process. For all runs, the electrolysis period was 30 minutes, and the pH was maintained at 7. To analyze the MG and MV removal efficiency (Re%), MINITAB-22 software was used. The scales for process variables were shown as low level (-1), center point (0), and high level (+1), whereas Table 2 shows the Box-Behnken design.

RESULTS AND DISCUSSION

Statistical analysis and regression model development

Table 3 displays dye removal efficiency and energy consumption (SEC), real and anticipated values data for the 15 batch runs, which were conducted based on Table 2, after 30 minutes of electrolysis and pH=7. A 59.4% dye removal efficiency was the lowest obtained value, and 96.6% was the greatest. The regression model equation in Equation 8 was attained using the MINITAB-22 software, and it illustrates the relationship between Re% and the studied parameters.

$$\begin{aligned}\text{Dye removal (Re\%)} = {} & 47.96 + 11.43\ C.D + \\ & +1.64\ Qa - 1.8\ NaCl\ conc. - 0.378\ C.D \times \\ & \times C.D - 0.910\ Qa \times Qa + 11.64\ NaCl\ conc. \times \\ & \times NaCl\ conc. + 0.404\ C.D \times Qa - 4.11\ C.D \times \\ & \times NaCl\ conc. + 3.12\ Qa \times NaCl\ conc.\end{aligned} \quad (8)$$

Variance analysis (ANOVA)

ANOVA was used to determine the acceptability of the BBD results. Additionally, it is an active method of system conceptualization and

Table 2. The box-Behnken design for removing dyes

Run	Code value			Actual value		
	X1	X2	X3	Current density (mA/cm^2), X1	NaCl concentration (g/L), X2	Air flow rate (L/min), X3
1	-1	-1	0	1	0.4	3
2	0	-1	1	3	0.4	5
3	1	1	0	5	1	3
4	0	0	0	3	0.7	3
5	0	1	-1	3	1	1
6	0	1	1	3	1	5
7	-1	0	-1	1	0.7	1
8	0	0	0	3	0.7	3
9	0	0	0	3	0.7	3
10	-1	0	1	1	0.7	5
11	1	0	1	5	0.7	5
12	0	-1	-1	3	0.4	1
13	1	-1	0	5	0.4	3
14	1	0	-1	5	0.7	1
15	-1	1	0	1	1	3

Table 3. Values for dyes Re% and consumed energy (SEC)

Exp. No.	C.D., mA/cm^2	NaCl conc., g/L	Air flow rate, Qa, L/min	Actual dye removal, %	Predicted dye removal, %	E, V	SEC (kWh/kg dyes)
1	1	0.4	3	60.740	60.196	2.63	8.243
2	3	0.4	5	71.797	72.808	3.88	25.624
3	5	1	3	96.608	97.1	4.64	60.438
4	3	0.7	3	81.591	81.578	3.67	38.130
5	3	1	1	82.478	81.42	4.22	61.969
6	3	1	5	84.812	83.468	5.21	52.311
7	1	0.7	1	64.684	63.896	2.32	8.637
8	3	0.7	3	81.716	81.578	3.87	38.130
9	3	0.7	3	81.510	81.578	3.87	38.130
10	1	0.7	5	59.477	58.968	2.21	10.919
11	5	0.7	5	91.454	92.188	5.78	104.332
12	3	0.4	1	76.962	78.248	3.70	48.277
13	5	0.4	3	96.538	95.116	5.22	69.224
14	5	0.7	1	89.845	90.652	4.66	75.109
15	1	1	3	70.277	72.044	2.43	8.828

optimization (Jasim and Salman, 2024). Table 4 reports the ANOVA statistical terms, including the degree of freedom (DF), the contribution percentage for each variable (contr.%), and the adjusted sum of the squares (Adj. SS, Adj. MS, and Sequential Sum of the Squares (Seq. SS). The Fisher value (F-value) and the probability value (P-value) can be used to estimate the model's relevance. The regression equation may sufficiently explain the variation in the response if the F-value is greater than 4, and the model is statistically significant if the P-value is less than 0.05 (Mohammed Ali and Salman, 2024).

The results in Table 4 demonstrate that the model for dye removal is highly significant, with an F and P value of 78.63, and 0.000, respectively and this model accurately describes the treatment process. The R^2 multiple correlation value was 0.9930, and the adjusted R^2 (0.9804) and predicted R^2 (0.8879) were very good. The current density had the greatest significant influence on the efficiency of dye elimination, followed by a moderate effect of NaCl concentration, with respective contribution percentages of 88.80% and 4.74%, respectively. In contrast, the flow rate had the lower influence, contributing to 0.28%.

Optimization and confirmation experiments

Optimizing several variables to obtain maximal removal with the lowest value of energy and expense is the primary objective of all electrochemical systems, which aim to treat wastewater and remove contaminants with the least amount of energy needed. To achieve this primary goal, MINITAB-22 was utilized to increase the desired function (DF) by controlling weight or importance, which is divided into five elements: minimum, maximum, nothing, in range, and the target (Chakawa et al., 2021; Heydan et al., 2024).

For the 3DECF process, the "maximum" dye removal target was set at DF = 1.0. The optimization procedure was carried out under the following limitations and variables; the results are shown in Tables 5 and 6. The lower limit value of dye removal was 59.477%, while the highest limit was 96.608%. Two confirmation runs were carried out at these optimal parameters to confirm that they can achieve the maximum value of dye removal efficiency, as displayed in Table 6. In addition, COD was measured under these optimal conditions before and after the experiment. It was (53) and (0) mg/L, respectively, which emphasizes the high efficiency of the 3DECF system in removing organic pollutants, not only color.

Effect of the factors studied on the Re%

A 3D surface plot with 2D plots was used to examine the synergistic effects of the factors under study and their influence on the response more thoroughly using RSM analysis, as shown in Figures 2 (a1, b1, a2, and b2).

Table 4. Analysis of variance for dyes Re%

Source	DF	Seq SS	Contribution	Adj SS	Adj MS	F-value	P-value
Model	9	2013.25	99.30%	2013.25	223.69	78.63	0.000
Linear	3	1902.30	93.83%	1902.30	634.10	222.88	0.000
C.D	1	1800.39	88.80%	1800.39	1800.39	632.83	0.000
Qa	1	5.74	0.28%	5.74	5.74	2.02	0.215
NaCl conc.	1	96.17	4.74%	96.17	96.17	33.80	0.002
Square	3	62.09	3.06%	62.09	20.70	7.27	0.028
C.D*C.D	1	6.58	0.32%	8.45	8.45	2.97	0.145
Qa*Qa	1	51.45	2.54%	48.96	48.96	17.21	0.009
NaCl conc.*NaCl conc.	1	4.05	0.20%	4.05	4.05	1.43	0.286
2-way interaction	3	48.86	2.41%	48.86	16.29	5.73	0.045
C.D*Qa	1	10.47	0.52%	10.47	10.47	3.68	0.113
C.D*NaCl conc.	1	24.34	1.20%	24.34	24.34	8.56	0.033
Qa*NaCl conc.	1	14.06	0.69%	14.06	14.06	4.94	0.077
Error	5	14.23	0.70%	14.23	2.85		
Lack-of-fit	3	14.20	0.70%	14.20	4.73	439.59	0.002
Pure error	2	0.02	0.00%	0.02	0.01		
Total	14	2027.48	100.00%				
Model summary	S	R-sq	R-sq(adj)	PRESS	R-sq(pred)	AICc	BIC
	1.6871	99.30%	98.04%	227.304	88.79%	151.77	71.56

Table 5. Optimal result for the maximum dye removal system for the actual result

Response	Goal	Lower	Target	Weight	Importance
Actual color removal, %	maximum	59.477	96.608	1	1

Table 6. Results for dye Re% and SEC at optimum conditions

Run No.	C.D. (mA/cm^2)	NaCl (g/L)	Q_a (L/min)	Time (min)	Dyes removal (%)	Average removal (%)	E (V)	SEC (kWh/kg of dyes)
1	5	1	3.7	30	92.670	93.151	4.75	67.847
2	5	1	3.7	30	93.632		4.63	67.967

The removal of dyes has been improved as the current density has increased, as shown in Figure 2 (a1, and b1). In addition, by comparing the results of experiments 1 and 13 as displayed in Table 3, a conclusion can be drawn easily, an increase in the current density from 1 to 5 mA/cm^2 within 30 minutes of electrolysis resulted an increase in the dyes removal% from 60.740 to 96.538% at a NaCl concentration of 0.4 g/L and an air flow rate of 3 L/min.

As the current density increases, more electrode ionic species are generated, based on Faraday's Equation [m = [ItM/zF]]. Ni^{+2} would be released from the anode, which would improve the removal of dyes by producing more $Ni(OH)_2$ flocs in the solution (Jasim and Salman, 2024; Abbas et al., 2022). Additionally, a higher current density would accelerate the formation of H_2 and O_2 bubbles, which have a significant effect on the mass transfer, flotation rate, and solution mixing of electrodes. As one of the crucial operational factors that must be considered when designing an EC setup, current density has a significant impact on the governing contaminant separation technique in addition to influencing system response time. To prevent a drop in current efficiency and electrical energy waste, this crucial parameter must be managed (Kul et al., 2020; Mohammed Ali and Salman, 2024).

As expected, the removal dye results showed an increase with rising air flow rate. It should be noted that at a NaCl concentration of 1 g/L, and 3 mA/cm^2, the removal increased slightly from 82.478% to 84.812 % as the air flow rate increased from 1 to 5 L/min within 30 min of treatment. However, it can be predicted from runs 5

and 6, while the removal dropped from 76.962 to 71.797 % of dye at 3 mA/cm², NaCl concentration 0.4 g/L, due to the increase in air flow rate from 1 to 5 L/min, respectively, as shown in experiments 2 and 12.

Small gas bubbles adhere to the suspended impurities in the liquid phase to create agglomerates with lower relative densities than the bulk solution, according to the fundamental idea of flotation. This density differential causes these flocs to rise quickly to the surface of the liquid, guaranteeing quicker removal rates in terms of efficiency and time (Abdulrazzaq et al., 2021). Good mixing and flotation are provided by moderate air flow, while at high air flow, bubbles collide and merge into larger ones. Large bubbles rise too fast and have less surface area to attach to dye flocs, so they are less effective for flotation, and strong air agitation breaks apart dye-coagulant flocs into smaller particles, which are harder to float or settle. Bubbles rise quickly at high flow, so there is less contact time for adsorption/floc-bubble attachment, and so many bubbles disturb the floated layer on top, reducing solid-liquid efficiency (Tchamango et al., 2010).

Figure 2 (a2, and b2) illustrates the impact of adding NaCl. Table 3 indicates that, when comparing the results of runs 1 and 15 at 1mA/cm² and 3 L/min air flow rate, the dye removal efficiency would increase from 60.740 to 70.277% if the concentration of electrolyte increased from 0.4 to 1 g/L.

The addition of various electrolytes, such as KCl, NaCl, and Na_2SO_4 has a direct impact on the effectiveness of the EC process. NaCl and Na_2SO_4 were selected as the primary electrolytes in this study, because it is naturally present in wastewater from a variety of industries, particularly the textile sector, where they are used as absorbents of dyes in fabric fibers in addition to their superior efficiency in raising the conductivity of the electrolytes (Jasim and Salman, 2024). Additionally, all wastewater types naturally contain Ca ions, which are prevented from being negatively charged by the presence of Cl ions (Mohammed et al., 2021). The addition of NaCl is therefore

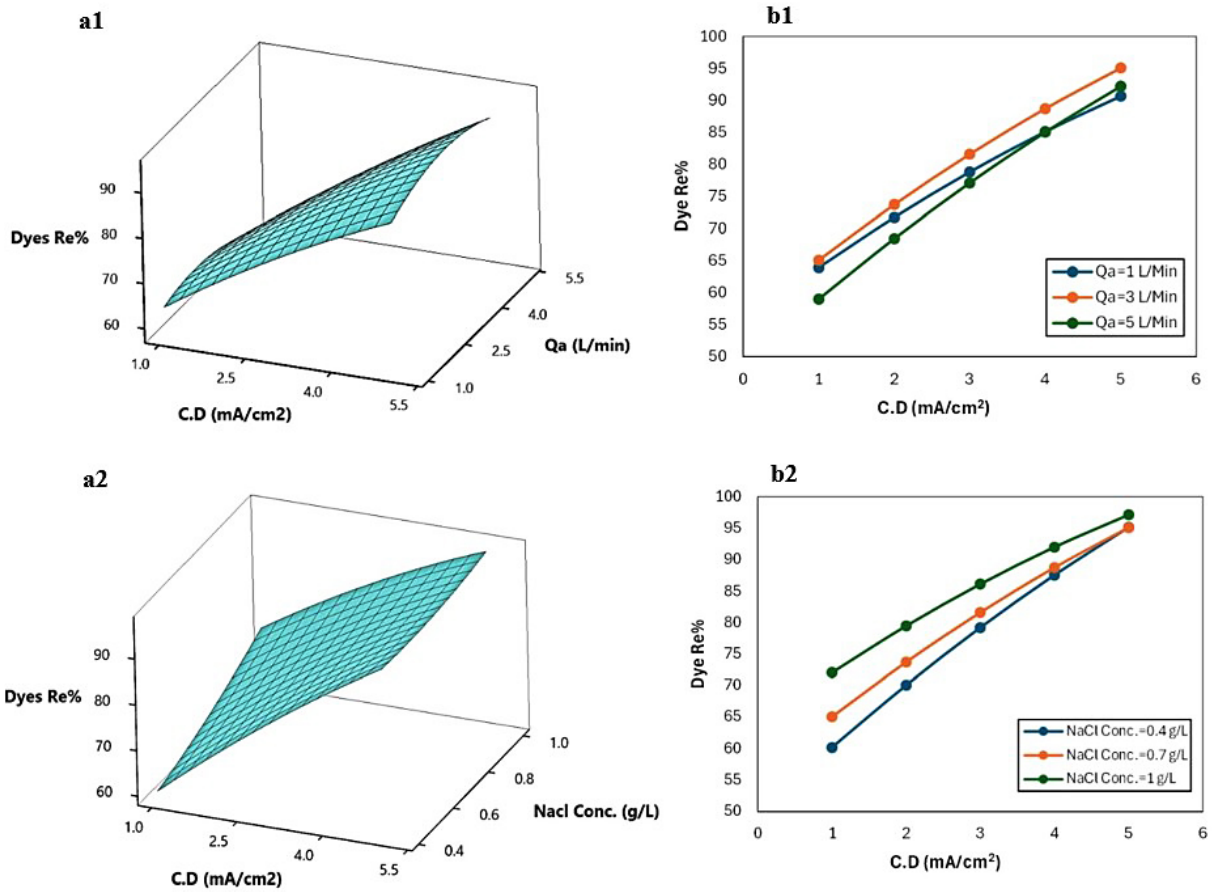

Figure 2. Effect of current density with NaCl concentration and air flow rate on dyes Re% at fixed NaCl conc. of 0.7 g/L, (a1) 3D surface plot, and (b1) 2D plot, and at fixed Qa=3 L/min. (a2) 3D surface plot, (b2) 2D plot

frequently regarded as one of the primary factors influencing the EC process efficiency. This is also explained by the fact that anodically producing chlorine species such as hypochlorous acid (HOCl) and hypochlorite ions ($^{-}$OCl) by adding NaCl to the bulk solution improves indirect electrolysis and converts organic contaminants into H_2O and CO_2 (Muthumanickam and Saravanathamizhan, 2021; Titchou et al., 2020). Equations (9-12), which involve adding NaCl to the bulk solution, describe the primary reactions (Jasim and Salman, 2024; Titchou et al., 2020). However, the primary chlorine species that would be generated in a neutral bulk solution is HOCl, which is more effective in removing contaminants than hypochlorite ions (Jasim and Salman, 2024).

$$2Cl^- \rightarrow 2Cl_2 + 2e^- \quad (9)$$

$$Cl_2 + H_2O \rightarrow HOCl + H^+ + Cl^- \quad (10)$$

$$HOCl \rightarrow H^+ + OCl^- \quad (11)$$

$$Dye + OCl^- \rightarrow Intermediates \rightarrow \rightarrow CO_{2(g)} + H_2O + Cl^- \quad (12)$$

As expected, the results in Table 3 showed that SEC values were increased in contrast with the current density. It can easily be emphasized that at 0.4 g/L of NaCl and after 30 min of treatment, the energy consumed was boosted from 8.243 to 69.224 kWh/kg of dyes as the C.D increased from 1 to 5 mA/cm². Nevertheless, as NaCl increased, SEC decreased. As it was shown in Table 3, runs 3 and 13 show that, during 30 minutes of electrolysis, SEC dropped from 69.224 to 60.438 kWh/kg of dye at 5 mA/cm², while the concentration of NaCl increased from 0.4 to 1 g/L, respectively. The explanation for this reduction in SEC with increasing NaCl concentration is due to the improvement in the electrolyte conductivity, which decreases the insulating layer of the anode, lowering the voltage, and consequently reducing SEC values (Irki et al., 2018).

Characterization of alum sludge

Figure 3 (a, and b) shows the EDX results for the alum sludge utilization as a third particle in the 3DECF system, before and after its utilization in the reaction. The metal Si had the most significant percentage of all metals that naturally presented in alum sludge with 17.7%, followed by 6.7% of Al and 4.0% of Fe, with minor components like Mg, Na, Ca, and K. Figure 3a showed that O had the highest weight percentage of composition, of 45.3%, followed by carbon 13.7%. After using the alum sludge in the 3DECF experiments, EDX analysis revealed a decrease in the percentage of both oxygen (24.2%) and aluminum (6.1%) elements, along with the appearance of Ni, confirming the elimination of leached Ni excess in the electrocoagulation reaction. Otherwise, there was an increase in each percentage of the silica (21%), carbon (19.3%), and iron (6.8%) elements.

Figure 4 (a1, b1, a2, and b2) represents the SEM analysis of the alum sludge calcined at

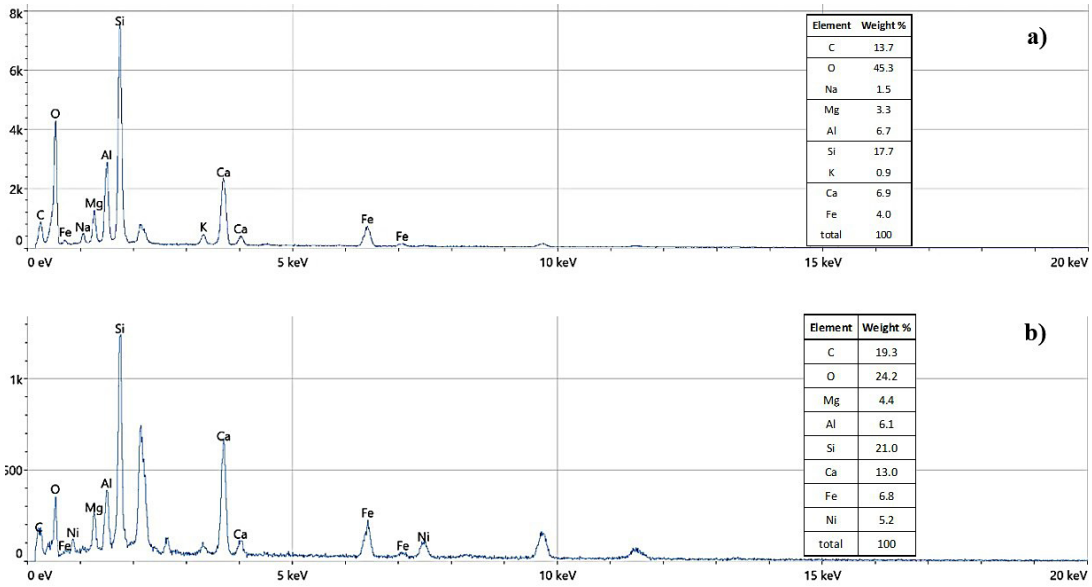

Figure 3. EDX images of alum sludge calcined: (a) before the process, and (b) after the process

600°C before and after being used as a 3rd particle in the 3DECF system. The morphological structure of Figure 4 illustrates a highly porous and uneven structure for alum sludge, characterized by agglomerates of varying particle sizes. The texture appears rough, because the surface is coated in tiny granular forms or micro-crystals. Porosity and high surface area promote the adsorption of dye molecules. Regeneration and reuse are made possible by the physical stability of alum sludge. Utilizing waste materials, such as alum sludge, in water treatment operations promotes sustainability by reducing waste disposal and enhancing color removal efficiency (Iwuozor et al., 2021).

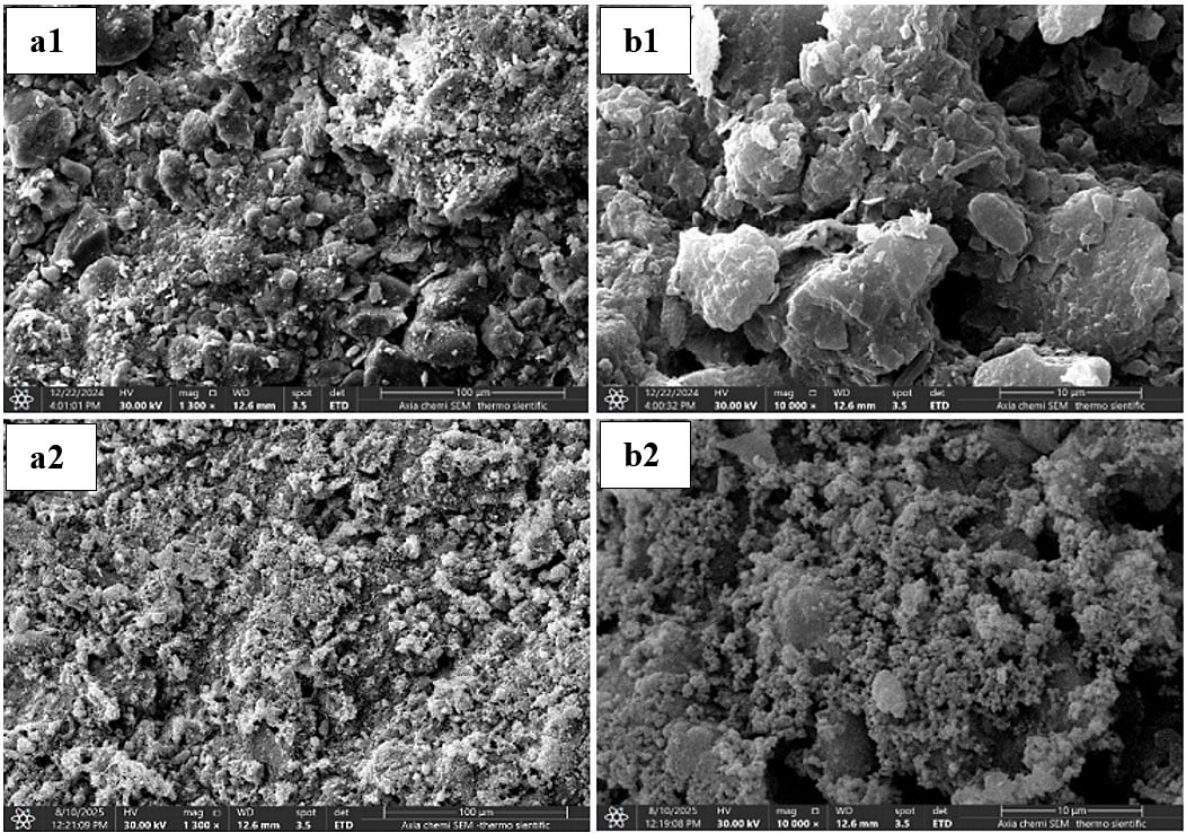

Figure 4. SEM images of alum sludge as 3rd particle at two magnifications (a represents 100 µm and b represents 10 µm); (1) before its utilization in the 3DECF system, and (2) after it

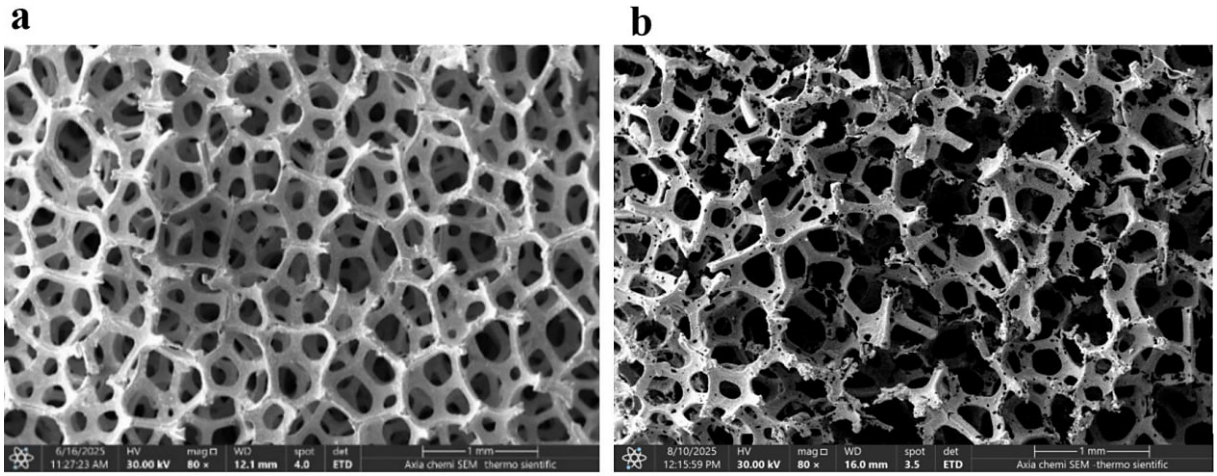

Figure 5. SEM image NiF electrode at various magnifications (a) before the 3DECF process (b) after the 3DECF process

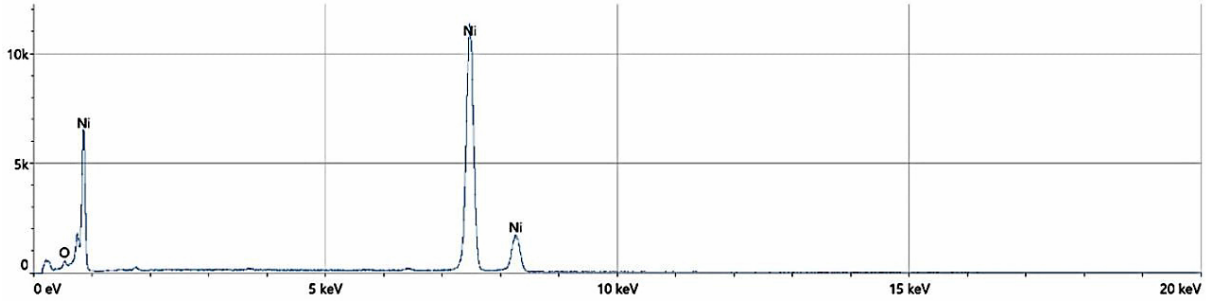

Figure 6. EDX image of NiF electrode

Characterizations of NiF

The morphological structure and element composition of NiF anode would be determined using SEM and EDX. Figure 5 shows the morphological structure of the NiF anode, before and after 15 3DECF operations. Before tests, Figure 5a displays the smooth surface, cross-linked, three-dimensional porous structure, and minimal diameter of the Ni foam. Due to the porous structure of NiF, it has a vast surface area, which may enhance the transfer of charges, strengthen the pseudo-capacitance properties, and eliminate the impediments between the electrolyte and active material (Salleh et al., 2020; Thwaini and Salman, 2023). Because of its three-dimensional structure, the NiF anode would improve solution mixing and H_2 gas production, which would increase flotation. After 15 experiments, the change in its surface, as shown in Figure 5b, is easily predicted in its structure as a result of the leaching and dissolution of Ni ions during the 3DECF runs.

The EDX performance of NiF anodes is shown in Figure 6. Ni is expected to have the largest share of the overall composition, as well as trace elements.

In spite of excellent results by utilizing NiF as an anode, as predicted from these results, it is worth remembering that Ni metal is non-biodegradable and among the most toxic heavy metals. The maximum allowable concentration of Ni in released industrial waste and drinking water is 2 and 0.1 mg/L, respectively, according to World Health Organization (WHO) guidelines (Muhammad et al., 2016). Therefore, the detection of the 3DECF system is not governed by its efficiency in removing contaminants but rather by the permissible concentration of Ni ions. The 3DECF system gave the highest dye removal efficiency at 5 mA/cm², but also with a high concentration of Ni, which is equal to 1.8 mg/L, while at 3 mA/cm², it is 0.7 mg/L, which can be considered within the limitations of WHO. Consequently, 3DECF can be operated to obtain a good percentage of dye removal efficiency with an allowable concentration of Ni ions.

CONCLUSIONS

In this study, a 3DECF electrocoagulation system was utilized to predict the removal of malachite green (MG) and methyl violet (MV) dyes, which was expected to improve when a 2D system was modified by adding a specific amount of alum sludge. Response surface methodology was applied to optimize the impact of air flow rate, current density, and NaCl concentration on the efficiency of the 3DECF system. The 3DECF process was shown to be impacted foremost by current density, then by NaCl concentration, and least affected by air flow rate.

Both the model and the empirical data showed a significant agreement, as indicated by the high R^2 value of 0.99230. The maximum removal effectiveness, which was achieved at 5 mA/cm² of current density, 1 g/L of NaCl, an air flow rate of 3.7 L/min, and 30 minutes of electrolysis time, was 93.151% with a power consumption of 67.847 kWh/kg of dyes. Utilizing the NiF electrode greatly enhanced the 3DECF process due to its high surface area, which promoted the formation of hydrogen and oxygen gases and, subsequently, improved mass transfer, solution mixing, and flotation rate. In the end, in comparison with previous studies, the 3DECF system, using NiF as the anode and a stainless-steel mesh cathode, with alum sludge as a third particle electrode is an efficient wastewater treatment method providing more effective dye elimination with less power consumption and fewer chemical components.

REFERENCES

1. Abbas, R. N., & Abbas, A. S. (2022). Kinetics and Energetic Parameters Study of Phenol Removal from Aqueous Solution by Electro-Fenton Advanced Oxidation Using Modified Electrodes with PbO_2 and Graphene. *Iraqi Journal of Chemical and Petroleum Engineering*, *23*(2), 1–8. https://doi.org/10.31699/IJCPE.2022.2.1
2. Abbas, S. H., Younis, Y. M., Rashid, K. H., & Khadom, A. A. (2022). Removal of methyl orange dye from simulated wastewater by electrocoagulation technique using Taguchi method: kinetics and optimization approaches. *Reaction Kinetics, Mechanisms and Catalysis*, *135*(5), 2663–2679. https://doi.org/10.1007/S11144-022-02269-9/METRICS
3. Abdulrazzaq, N. N., Al-Sabbagh, B. H., & Shanshool, H. A. (2021). Coupling of electrocoagulation and microflotation for the removal of textile dyes from aqueous solutions. *Journal of Water Process Engineering*, *40*, 101906. https://doi.org/10.1016/J.JWPE.2020.101906
4. Ahmad, A., Abdullah, S. R. S., Hasan, H. A., Othman, A. R., & Kurniawan, S. B. (2024). Aquaculture wastewater treatment using plant-based coagulants: Evaluating removal efficiency through the coagulation-flocculation process. *Results in Chemistry*, *7*, 101390. https://doi.org/10.1016/J.RECHEM.2024.101390
5. Akhtar, M., Sarfraz, M., & Ahmad, M. (2025). Use of low-cost adsorbent for waste water treatment: Recent progress, new trend and future perspectives. *Desalination and Water Treatment*, *321*, 100914. https://doi.org/10.1016/J.DWT.2024.100914
6. Alegbe, E. O., & Uthman, T. O. (2024). A review of history, properties, classification, applications and challenges of natural and synthetic dyes. *Heliyon*, *10*(13), e33646. https://doi.org/10.1016/J.HELIYON.2024.E33646/ASSET/060DF4A4-09C9-4E4A-8E6B-93F760CF4D20/MAIN.ASSETS/GR2.JPG
7. Amalina, F., Razak, A. S. A., Krishnan, S., Zularisam, A. W., & Nasrullah, M. (2022). Dyes removal from textile wastewater by agricultural waste as an absorbent – A review. *Cleaner Waste Systems*, *3*, 100051. https://doi.org/10.1016/J.CLWAS.2022.100051
8. Anbia, M., Mohammadi, N., & Mohammadi, K. (2010). Fast and efficient mesoporous adsorbents for the separation of toxic compounds from aqueous media. *Journal of Hazardous Materials*, *176*(1–3), 965–972. https://doi.org/10.1016/J.JHAZMAT.2009.11.135
9. Askari, R., Mohammadi, F., Moharrami, A., Afshin, S., Rashtbari, Y., Vosoughi, M., & Dargahi, A. (2023). Synthesis of activated carbon from cherry tree waste and its application in removing cationic red 14 dye from aqueous environments. *Applied Water Science*, *13*(4), 1–12. https://doi.org/10.1007/S13201-023-01899-1/FIGURES/6
10. Chakawa, S., Aziz, M., Libralato, G., & Stefanakis, A. I. (2021). *Investigating the Result of Current Density, Temperature, and Electrolyte Concentration on COD: Subtraction of Petroleum Refinery Wastewater Using Response Surface Methodology*. https://doi.org/10.3390/w13060835
11. Chen, M., Heijman, S. G. J., & Rietveld, L. C. (2024). Ceramic membrane filtration for oily wastewater treatment: Basics, membrane fouling and fouling control. *Desalination*, *583*, 117727. https://doi.org/10.1016/J.DESAL.2024.117727
12. Chen, S., Qin, C., Wang, T., Chen, F., Li, X., Hou, H., & Zhou, M. (2019). Study on the adsorption of dyestuffs with different properties by sludge-rice husk biochar: Adsorption capacity, isotherm, kinetic, thermodynamics and mechanism. *Journal of Molecular Liquids*, *285*, 62–74. https://doi.org/10.1016/J.MOLLIQ.2019.04.035
13. Crini, G., & Lichtfouse, E. (2019). Advantages and disadvantages of techniques used for wastewater treatment. *Environmental Chemistry Letters*, *17*(1), 145–155. https://doi.org/10.1007/S10311-018-0785-9/METRICS
14. Das, S., Cherwoo, L., & Singh, R. (2023). Decoding dye degradation: Microbial remediation of textile industry effluents. *Biotechnology Notes*, *4*, 64–76. https://doi.org/10.1016/J.BIOTNO.2023.10.001
15. Derakhshan, A., Rezaei Kalantari, R., Farzadkia, M., Tiyuri, A., & Esrafili, A. (2023). The effect of biological treatment methods on the concentration of carbonaceous pollutants in the slaughterhouse wastewater: A systematic review. *Case Studies in Chemical and Environmental Engineering*, *8*, 100451. https://doi.org/10.1016/J.CSCEE.2023.100451
16. Hasnaoui, A., Chikhi, M., Balaska, F., Seraghni, W., Boussemghoune, M., & Dizge, N. (2024). Electrocoagulation employing recycled aluminum electrodes for methylene blue remediation. *Desalination and Water Treatment*, *319*, 100453. https://doi.org/10.1016/J.DWT.2024.100453
17. Hsini, A., Naciri, Y., Laabd, M., El Ouardi, M., Ajmal, Z., Lakhmiri, R., Boukherroub, R., & Albourine, A. (2020). Synthesis and characterization of arginine-doped polyaniline/walnut shell hybrid composite with superior clean-up ability for chromium (VI) from aqueous media: Equilibrium, reusability and process optimization. *Journal of Molecular Liquids*, *316*, 113832. https://doi.org/10.1016/J.MOLLIQ.2020.113832
18. Irki, S., Ghernaout, D., Naceur, W., Alghamdi, A., & Aichouni, M. (2018). Decolorizing Methyl Orange by Fe-Electrocoagulation Process-A Mechanistic

Insight. *International Journal of Environmental Chemistry*, *2*, 18–28. https://doi.org/10.11648/j.ijec.20180201.14

19. Islam, S. M. D. U. (2017). Electrocoagulation (EC) technology for wastewater treatment and pollutants removal. *Sustainable Water Resources Management 2017 5:1*, *5*(1), 359–380. https://doi.org/10.1007/S40899-017-0152-1
20. Ismail, G. A., & Sakai, H. (2022). Review on effect of different type of dyes on advanced oxidation processes (AOPs) for textile color removal. *Chemosphere*, *291*, 132906. https://doi.org/10.1016/J.CHEMOSPHERE.2021.132906
21. Iwuozor, K. O., Ighalo, J. O., Emenike, E. C., Igwegbe, C. A., & Adeniyi, A. G. (2021). Do adsorbent pore size and specific surface area affect the kinetics of methyl orange aqueous phase adsorption? *Journal of Chemistry Letters*, *2*(4), 188–198. https://doi.org/10.22034/JCHEMLETT.2022.327407.1048
22. Jasim, A. Q., & Ajjam, S. K. (2024). Removal of heavy metal ions from wastewater using ion exchange resin in a batch process with kinetic isotherm. *South African Journal of Chemical Engineering*, *49*, 43–54. https://doi.org/10.1016/J.SAJCE.2024.04.002
23. Jasim, R. A., & Salman, R. H. (2024). Congo red removal from aqueous solution by electrocoagulation- electro-oxidation combined system with Al and Cu–Mn–Ni nano composite as efficient electrodes. *Case Studies in Chemical and Environmental Engineering*, *9*, 100747. https://doi.org/10.1016/J.CSCEE.2024.100747
24. Jawad, N. A., & Naife, T. M. (2022). Mathematical Modeling and Kinetics of Removing Metal Ions from Industrial Wastewater. *Iraqi Journal of Chemical and Petroleum Engineering*, *23*(4), 59–69. https://doi.org/10.31699/IJCPE.2022.4.8
25. Jo, J. Y., Choi, J. H., Tsang, Y. F., & Baek, K. (2021). Pelletized adsorbent of alum sludge and bentonite for removal of arsenic. *Environmental Pollution*, *277*, 116747. https://doi.org/10.1016/J.ENVPOL.2021.116747
26. Kul, M., Oskay, K. O., Erden, F., Akça, E., Katirci, R., Köksal, E., & Akinci, E. (2020). Effect of Process Parameters on the Electrodeposition of Zinc on 1010 Steel: Central Composite Design Optimization. *International Journal of Electrochemical Science*, *15*(10), 9779–9795. https://doi.org/10.20964/2020.10.19
27. Kumar, R., Kang, C. U., Mohan, D., Khan, M. A., Lee, J. H., Lee, S. S., & Jeon, B. H. (2020). Waste sludge derived adsorbents for arsenate removal from water. *Chemosphere*, *239*, 124832. https://doi.org/10.1016/J.CHEMOSPHERE.2019.124832
28. Lichtmannegger, T., Hell, M., Wehner, M., Ebner, C., & Bockreis, A. (2024). Seasonal tourism's impact on wastewater composition: Evaluating the potential of alternating activated adsorption in primary treatment. *Science of The Total Environment*, *926*, 171869. https://doi.org/10.1016/J.SCITOTENV.2024.171869
29. Mohammed Ali, A. T., & Salman, R. H. (2024). Enhancing the Removal of Methyl Orange Dye by Electrocoagulation System with Nickel Foam Electrode – Optimization with Surface Response Methodology. *Journal of Ecological Engineering*, *25*(12), 26–38. https://doi.org/10.12911/22998993/193587
30. Mohammed, S. J., M-Ridha, M. J., Abed, K. M., & Elgharbawy, A. A. M. (2021). Removal of levofloxacin and ciprofloxacin from aqueous solutions and an economic evaluation using the electrocoagulation process. *International Journal of Environmental Analytical Chemistry*, *103*(16), 3801–3819. https://doi.org/10.1080/03067319.2021.1913733;PAGE:STRING:ARTICLE/CHAPTER
31. Muhammad, H. N., Mahmud, E., Obidul Huq, A. K., & Binti Yahya, R. (2016). *The removal of heavy metal ions from wastewater/ aqueous solution using polypyrrole-based adsorbents: a review*. https://doi.org/10.1039/c5ra24358k
32. Muthumanickam, K., & Saravanathamizhan, R. (2021). Electrochemical treatment of dye wastewater using nickel foam electrode. *J. Electrochem. Sci. Eng*, *11*(3), 209–215. https://doi.org/10.5599/jese.1011
33. Najim, A. A., & Mohammed, A. A. (2018). Biosorption of Methylene Blue from Aqueous Solution Using Mixed Algae. *Iraqi Journal of Chemical and Petroleum Engineering*, *19*(4), 1–11. https://doi.org/10.31699/IJCPE.2018.4.1
34. Nguyen, M. D., Donaldson, D., Adhikari, S., Amini, N., Mallya, D. S., Thomas, M., Moon, E. M., & Milne, N. A. (2023). Phosphorus adsorption and organic release from dried and thermally treated water treatment sludge. *Environmental Research*, *234*, 116524. https://doi.org/10.1016/J.ENVRES.2023.116524
35. Oh, M., Lee, K., Jeon, M. K., Foster, R. I., & Lee, C. H. (2023). Chemical precipitation–based treatment of acidic wastewater generated by chemical decontamination of radioactive concrete. *Journal of Environmental Chemical Engineering*, *11*(5), 110306. https://doi.org/10.1016/J.JECE.2023.110306
36. Qadeer, A., Saqib, Z. A., Ajmal, Z., Xing, C., Khan Khalil, S., Usman, M., Huang, Y., Bashir, S., Ahmad, Z., Ahmed, S., Thebo, K. H., & Liu, M. (2020). Concentrations, pollution indices and health risk assessment of heavy metals in road dust from two urbanized cities of Pakistan: Comparing two sampling methods for heavy metals concentration. *Sustainable Cities and Society*, *53*, 101959. https://doi.org/10.1016/J.SCS.2019.101959

37. Salleh, N. A., Kheawhom, S., & Mohamad, A. A. (2020). Characterizations of nickel mesh and nickel foam current collectors for supercapacitor application. *Arabian Journal of Chemistry*, *13*(8), 6838–6846. https://doi.org/10.1016/J.ARABJC.2020.06.036
38. Samuchiwal, S., Gola, D., & Malik, A. (2021). Decolourization of textile effluent using native microbial consortium enriched from textile industry effluent. *Journal of Hazardous Materials*, *402*, 123835. https://doi.org/10.1016/J.JHAZMAT.2020.123835
39. Seidmohammadi, A., Asgari, G., Dargahi, A., Leili, M., Vaziri, Y., Hayati, B., Shekarchi, A. A., Mobarakian, A., Bagheri, A., Nazari Khanghah, S. B., & Keshavarzpour, A. (2019). A Comparative Study for the Removal of Methylene Blue Dye from Aqueous Solution by Novel Activated Carbon Based Adsorbents. *Progress in Color, Colorants and Coatings*, *12*(3), 133–144. https://doi.org/10.30509/PCCC.2019.81551
40. Tchamango, S., Nanseu-Njiki, C. P., Ngameni, E., Hadjiev, D., & Darchen, A. (2010). Treatment of dairy effluents by electrocoagulation using aluminium electrodes. *Science of The Total Environment*, *408*(4), 947–952. https://doi.org/10.1016/J.SCITOTENV.2009.10.026
41. Theydan, S. K., Mohammed, W. T., & Haque, S. M. (2024). Three-dimensional Electrocoagulation Process Optimization Employing Response Surface Methodology that Operated at Batch Recirculation Mode for Treatment Refinery Wastewaters. *Iraqi Journal of Chemical and Petroleum Engineering*, *25*(1), 59–74. https://doi.org/10.31699/ijcpe.2024.1.6
42. Thwaini, H. H., & Salman, R. H. (2023). Modification of Electro-Fenton Process with Granular Activated Carbon for Phenol Degradation – Optimization by Response Surface Methodology. *Journal of Ecological Engineering*, *24*(9), 92–104. https://doi.org/10.12911/22998993/168411
43. Titchou, F. E., Afanga, H., Zazou, H., Ait Akbour, R., & Hamdani, M. (2020). Batch elimination of cationic dye from aqueous solution by electrocoagulation process. *Mediterranean Journal of Chemistry*, *10*(1), 1–12. https://doi.org/10.13171/MJC10102001201163MH
44. Waghchaure, R. H., Adole, V. A., Kushare, S. S., Shinde, R. A., & Jagdale, B. S. (2023). Visible light prompted and modified ZnO catalyzed rapid and efficient removal of hazardous crystal violet dye from aqueous solution: A systematic experimental study. *Results in Chemistry*, *5*, 100773. https://doi.org/10.1016/J.RECHEM.2023.100773
45. Zhou, Y. F., & Haynes, R. J. (2010). Water Treatment Sludge Can Be Used As An Adsorbent For Heavy Metals In Wastewater Streams. *WIT Transactions on Ecology and the Environment*, *140*, 379–389. https://doi.org/10.2495/WM100341